

See discussions, stats, and author profiles for this publication at: <https://www.researchgate.net/publication/316782527>

Synthesis, quantum chemical computations and x-ray crystallographic studies of a new complex based of manganese (+II)

Article in Journal of Applied and Fundamental Sciences · May 2017

DOI: 10.4314/jfas.v9i2.11

CITATIONS

0

READS

288

5 authors, including:



Amel Messai

Abbes Laghrour - Khenchela University

35 PUBLICATIONS 106 CITATIONS

[SEE PROFILE](#)



Touhami Lanez

El-Oued University

229 PUBLICATIONS 915 CITATIONS

[SEE PROFILE](#)



Koray Sayin

Sivas Cumhuriyet University

126 PUBLICATIONS 1,575 CITATIONS

[SEE PROFILE](#)

Some of the authors of this publication are also working on these related projects:



Estimating the binding parameters of interaction between DNA with ferrocene derivatives using Voltammetric and UV/vis Spectroscopic techniques then confirmed by Docking simulation methods [View project](#)



Synthesis, characterisation, anti-inflammatory, antidiabetic and antibacterial activities, ADMET analysis, in silico toxicity prediction, and molecular docking study of substituted N-ferrocenylmethylmethylaniline [View project](#)

SYNTHESIS, QUANTUM CHEMICAL COMPUTATIONS AND X-RAY
CRYSTALLOGRAPHIC STUDIES OF A NEW COMPLEX BASED
OF MANGANESE (+II)

N. Benyza^{1,2*}, A. Messai¹, A. Hamdaoui¹, T. Lanez² and K. Sayin³

¹Laboratoire d'Ingénierie et Sciences des Matériaux Avancés (ISMA) Institut des Sciences et Technologie Université Abbés Laghrour Khenchela ; 40000, Algeria

²VTRS Laboratory, Department of Chemistry, Faculty of Exact Sciences, University of El-Oued, PO Box 789, El-Oued 39000, Algeria

³Department of Chemistry, Institute of Science, Cumhuriyet University 58140 Sivas – Turkey

Received: 30 January 2017 / Accepted: 25 April 2017 / Published online: 01 May 2017

ABSTRACT

The ligand oxime, $C_7H_9N_5O_2$, was Synthesis and characterises with different characterization methods such as 1H NMR and FTIR spectroscopy. The complexation of this ligand with manganese (II) perchlorate yielded pink crystals of formula $[Mn (C_7H_9N_5O_2)_2]^{2+}$, $2[ClO_4]^-$, which crystallized in the monoclinic space group $P2_1/n$ with $a = 12.824(3)$, $b=13.799(2)$, $c=15.441(4)\text{Å}$, $\beta = 100.17(2)$, and $Z = 4$. The complex consists of cations (+II) and two perchlorate anions, the cations part existing in a slightly distorted octahedral complex. Computational investigations of manganese (II) complex are done by using the DFTmethod with B3LYP functional in conjunction with the 6-31G(d,p) and lanl2dz basis sets in the gas phase imposing the C_1 and C_{2v} symmetries.

Keywords: Manganese complex; Crystal structure; DFT method; B3LYP functional; 6-31G(d,p) and (LANL2DZ) basis.

Author Correspondence, e-mail: nabsat1979@yahoo.fr

doi:<http://dx.doi.org/10.4314/jfas.v9i2.11>



1. INTRODUCTION

The chemistry of oxime-based ligand is diverse [1]. Introduced first in 1905 by Tschugaeff [2], e.g. preparation of nickel (II) dimethylglyoximate and recognition of the chelate five-membered character of this complex by Chugaev [3-4], the oximes as potential ligands have been increasingly expanding its horizon in coordination chemistry. Stability structure and reactivity of molecules, analytical and organometallic chemistry and particularly syntheses of molecules with unusual electronic properties are the aspects that kindled the interest for the oxime-based ligands [5-9]. Oxime ligands are used to obtain polynuclear compounds with molecular magnetism and supramolecular structure. Due to their ability to form bridges with metal ions [10, 11]. Also; the presence of additional donor group together with the oxime group in the ligand molecule resulting a significant increase in chelating efficiency and ability to form polynuclear complexes [12].

The literature contains reports of some amide oximes which can co-ordinate as bi-,tri-tetra-and hexa-dentate ligands [13-18]. The majority of these oximes are aliphatic compounds which form five-membered rings utilizing the diimine moiety, $-N=C-C=N-$, involving oxime and imine nitrogens as the co-ordination sites with transition-metal atoms [19].

Pyridine-2,6-dicarboxamide oxime (pyridine-2,6-diamidoxime), $C_7H_9N_5O_2$ (L), possesses the structural requirements to react as a polydentate ligand with the heterocyclic and two oxime nitrogen atoms forming five-membered rings with metal ions [20].

This research was carried out with the specific purpose of determining the structures of manganese (+II) co-ordination with pyridine-2,6-dicarboxamide oxime. We report here the synthesis, the single crystal X-ray structure of the complex and the Optimization of the structure using DFT method with B3LYP functional at 6-31G (d,p) and (LANL2DZ) levels in vacuo.

2. RESULTS AND DISCUSSION

The crystal structure of $[Mn(L)_2^{+2}, 2(ClO_4)^-]$ has been reported and discussed with X-ray single crystal data, the hydrogen-bonding networks has been also studied. Followed with a

quantum chemical computations of the geometrical parameters of our compound and compared with experimental results.

2.1. Synthesis

The ligand (**L**) pyridine-2,6-diamidoxime has been prepared as well as [19-20] by the reaction of 2,6-dicyanopyridine solution with a neutralized aqueous solution of hydroxylamine hydrochloride. The ^1H NMR shifts and the infrared spectrum bands are listed in the Experimental section.

Reaction of (**L**) with the manganese perchlorate in alcohol gave the corresponding coordination complex in 83.5% yield.

2.2 Structure

Crystals of complex suitable for X-ray study were grown by slow evaporation from alcoholic solution, a summary of crystal data and parameters for structure refinement details are given in Table 1. The atomic coordinates and equivalent thermal parameters are also given in Table 2.

Table 1. Crystal data and parameters for structure refinement

Crystal data	Complex
Empirical formula	MnC ₁₄ H ₈ Cl ₂ N ₁₀ O ₁₂ (a)
Formula weight (g mol ⁻¹)	<i>Mr</i> = 634.14
Temperature (K)	293
Crystal system	Monoclinic
Space group C2/c	<i>p</i> 2 ₁ / <i>n</i>
Hall symbo	-P 2yn
Unit cell dimensions (Å°)	
a	12.824(3)
b	13.799(2)
c	15.441(4)
°	114.691(19)
Volume (Å ³)	100.17(2)
Z ^a	4
Calculated density (g/cm ³)	1.566
Absorption coefficient (mm ⁻¹)	0.763
F(000)	1268
Crystal size (mm ³)	0.05 × 0.02 × 0.01 mm
Color	pink
Shape	Block
Cell parameters from	13138 reflections
Wavelength (Mo Ka) (Å)	0.71073
max - min	29.27° - 2.95°
Independent reflections	6163
reflections with <i>I</i> > 2 (<i>I</i>)	3734
Rint	0.0237
Limiting indices	
h	-12 17
k	<i>k</i> = -16 17
l	<i>l</i> = -20 17
Refinement method	Full-matrix Least-squares on F ²
Final R indices ^b [<i>F</i> ² > 2 (<i>F</i> ²)] R1, wR2	0.11, 0.26
Goodness-of-fit on F ² ^c	1.031
parameters	309
H atoms	
Largest difference peak and hole (e Å ⁻³)	a constrained refinement
max, min	0.952e, -1.168e

(a) The asymmetric unit contains 0.5 of the chemical formula.
(b) R1 = Σ|F_o - F_c|/ΣF_o. wR2 = {Σ[w(F_o² - F_c²)²]/Σ[w(F_o²)²]}^{1/2}.
(c) S = {Σ[w(F_o² - F_c²)²]/(Nobs - Nvar)}^{1/2}.

Table 2. Coordinates and Equivalent Isotropic Displacements Parameters of the non-Hydrogen atoms (\AA^2)

Atoms	x	Y	Z	U(eq) [\AA^2]
Mn1	0.69214(7)	0.17201(6)	0.37950(6)	0.0457(3)
O1	0.6167(7)	-0.1819(5)	0.4165(8)	0.155(5)
O2	1.01865	0.37493	0.34749	0.1859
O3	0.6701(7)	0.3071(8)	0.6875(5)	0.146(4)
O4	0.4486(8)	0.1618(5)	0.0765(5)	0.136(4)
N1	0.71921	-0.14080	0.40660	0.0586
N2	0.6513(4)	0.0165(3)	0.3999(4)	0.0534(19)
N3	0.8377(3)	0.0833(3)	0.3808(3)	0.0443(14)
N4	0.8303(4)	0.2703(3)	0.3581(4)	0.0560(19)
N5	1.01210	0.27074	0.35422	0.0654
N6	0.59613	0.32632	0.60060	0.0530
N7	0.6898(4)	0.2251(3)	0.5189(3)	0.0520(17)
N8	0.5551(3)	0.2693(3)	0.3769(3)	0.0418(14)
N9	0.5980(4)	0.1760(4)	0.2420(4)	0.0549(17)
N10	0.43949	0.22942	0.15756	0.0429
C1	0.72140	-0.04711	0.39951	0.0531(19)
C2	0.8313(4)	-0.0125(4)	0.3919(4)	0.0466(19)
C3	0.9189(5)	-0.0713(5)	0.3933(5)	0.062(2)
C4	1.0135(5)	-0.0276(5)	0.3863(5)	0.066(2)
C5	1.0208(5)	0.0692(5)	0.3764(5)	0.061(2)
C6	0.9274(4)	0.1243(4)	0.3717(4)	0.0480(19)
C7	0.92061	0.23310	0.36019	0.0546(19)
C8	0.6181(5)	0.2854(4)	0.5274(4)	0.0483(17)
C9	0.5395(4)	0.3142(4)	0.4497(4)	0.0427(16)
C10	0.4578(5)	0.3789(4)	0.4505(5)	0.056(2)
C11	0.3887(5)	0.3953(5)	0.3716(5)	0.063(3)
C12	0.4019(5)	0.3459(4)	0.2976(5)	0.0568(19)
C13	0.4869(4)	0.2836(4)	0.3023(4)	0.0435(17)
C14	0.5129(4)	0.2225(4)	0.2295(4)	0.0453(17)
Cl1	0.34134(13)	0.01791(13)	0.34301(13)	0.0665(6)
O5	0.2503(6)	-0.0238(9)	0.3599(8)	0.186(5)
O6	0.4248(6)	-0.0199(12)	0.4012(9)	0.252(8)
O7	0.3572(10)	0.0358(9)	0.2616(8)	0.205(7)
O8	0.3236(17)	0.1101(7)	0.3654(9)	0.277(11)
Cl2	0.76270(18)	0.02657(13)	0.10933(16)	0.0781(8)
O9	0.7095(10)	-0.0123(6)	0.1698(8)	0.199(6)
O10	0.7696(9)	-0.0338(5)	0.0380(6)	0.146(4)
O11	0.8645(8)	0.0548(9)	0.1444(8)	0.189(6)
O12	0.7219(12)	0.1153(7)	0.0887(9)	0.220(8)

The reaction of manganese (II) perchlorate with pyridine-2,6-dicarboxamide oxime produced a pink 1:2 complex (**1**), the crystal structure of this complex confirms the 1:2 Mn^{II} ligand co-ordination where the perchlorates anions are not involved in the co-ordination.

The complex crystallizes in the monoclinic space group $P2_1/n$ with the unit cell parameters $a = 12.824(3)\text{Å}$, $b = 13.799(2)\text{Å}$, $c = 15.441(4)\text{Å}$ and $\beta = 114.691(19)^\circ$. with four molecules in the unit cell (one per asymmetric unit). The asymmetric unit, formed by one Mn^{2+} metal ion, two crystallographically independent oxime ligands and two perchlorate counter-ion located on general positions. The molecular structure of the compound showing the atom numbering scheme is shown in Figure. 1

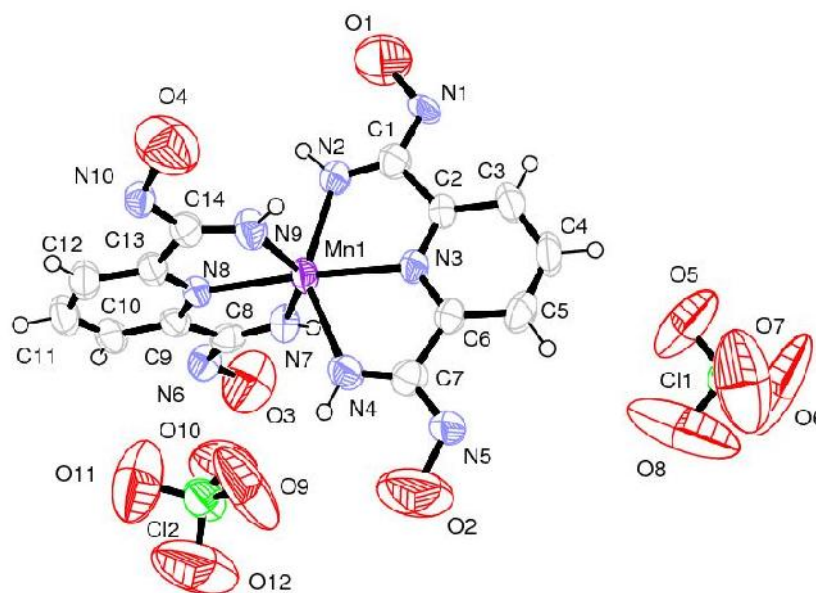


Fig.1. The molecular structure of the complex $\text{Mn}(\text{L})_2$

Manganese (II) ion is six-co-ordinated through the amine and heterocyclic nitrogens of the two oxime molecules. The resulting complex is the slightly distorted octahedron, caused by non-equivalent Mn-N bond length (Table 3 and 4). The two Mn-N (imine) bond lengths are almost equivalent, but shorter than the four Ni-N (amine) which are not mutually equivalent.

The two co-ordinated oximes are at 85.28° are almost orthogonal to each other. A comparison of the same bond lengths and angles for the free ligand and the manganese (II) complex shows little change in (L) and (1)[21].

Table 3. Experimental and calculated bond lengths (Å) of Mn(II) complex by using DFT/UB3LYP/LanL2DZ method

Bonds	Exp	Calculated Sym C _{2v}	Calculated Sym C ₁	Bonds	Exp	Calculated Sym C _{2v}	Calculated Sym C ₁
Mn-N ₂	2.254	2.295	2.196	N ₈ -C ₁₃	1.331	1.358	1.365
Mn-N ₃	2.210	2.260	2.265	N ₉ -C ₁₄	1.243	1.307	1.308
Mn-N ₄	2.289	2.295	2.313	N ₁₀ -C ₁₄	1.317	1.405	1.297
Mn-N ₇	2.292	2.311	2.303	C ₁₄ -C ₁₃	1.498	1.476	1.481
Mn-N ₈	2.225	2.261	2.256	C ₁₀ -C ₉	1.413	1.406	1.441
Mn-N ₉	2.239	2.311	2.139	C ₁₀ -C ₁₁	1.353	1.415	1.474
N ₂ -C ₁	1.260	1.314	1.362	C ₁₂ -C ₁₃	1.391	1.406	1.425
N ₃ -C ₂	1.334	1.364	1.362	C ₃ -C ₄	1.373	1.412	1.399
N ₃ -C ₆	1.326	1.364	1.359	C ₄ -C ₅	1.397	1.412	1.424
N ₁ -C ₁	1.331	1.392	1.351	C ₅ -C ₆	1.375	1.408	1.408
N ₄ -C ₇	1.251	1.314	1.339	N ₅ -O ₂	1.422	1.444	1.387
N ₅ -C ₇	1.336	1.392	1.370	N ₁ -O ₁	1.464	1.444	1.404
N ₆ -C ₈	1.330	1.405	1.350	N ₆ -O ₃	1.433	1.411	1.450
N ₇ -C ₈	1.260	1.307	1.296	N ₁₀ -O ₄	1.454	1.411	1.421
N ₈ -C ₉	1.317	1.358	1.341				

Table 4. Experimental and Calculated angles (deg.) of Mn(II) complex by using DFT/UB3LYP/LanL2DZ method

Angels	Exp	Calc Sym C _{2v}	Calc Sym C ₁	Angels	Exp	Calc Sym C _{2v}	Calc Sym C ₁
N ₂ -Mn-N ₃	071.39	078.58	075.90	Mn-N ₃ -C ₂	120.20	119.33	121.30
N ₂ -Mn-N ₄	142.11	147.17	149.20	Mn-N ₃ -C ₆	120.40	119.33	120.09
N ₂ -Mn-N ₉	093.01	092.17	091.50	Mn-N ₄ -C ₇	116.50	116.11	117.21
N ₂ -Mn-N ₈	109.00	101.41	108.70	C ₁ -C ₂ -N ₃	111.80	109.50	110.50
N ₂ -Mn-N ₇	098.84	092.17	090.40	N ₃ -C ₆ -C ₇	112.40	109.50	108.59
N ₃ -Mn-N ₄	070.89	078.58	077.40	Mn-N ₉ -C ₁₄	118.80	115.13	114.15
N ₃ -Mn-N ₇	105.75	101.06	102.60	Mn-N ₈ -C ₁₃	118.60	118.83	119.03
N ₃ -Mn-N ₈	176.11	180.00	170.90	Mn-N ₈ -C ₉	120.60	118.83	120.73
N ₃ -Mn-N ₉	112.44	101.06	100.16	Mn-N ₇ -C ₈	118.10	115.13	117.33
N ₄ -Mn-N ₇	094.63	092.17	93.30	C ₁₄ -C ₁₃ -N ₈	113.00	110.03	111.09
N ₄ -Mn-N ₈	108.87	101.41	102.10	N ₈ -C ₉ -C ₈	113.30	110.03	111.93
N ₄ -Mn-N ₉	097.90	092.17	098.40	C ₂ -C ₃ -C ₄	118.70	118.14	117.10
N ₇ -Mn-N ₈	070.37	078.93	078.10	C ₃ -C ₄ -C ₅	119.30	120.60	119.99
N ₇ -Mn-N ₉	141.81	147.87	141.90	C ₆ -N ₃ -C ₂	119.40	121.32	120.52
N ₈ -Mn-N ₉	071.44	078.93	074.50	C ₁₃ -N ₈ -C ₉	120.70	122.33	123.03
Mn-N ₂ -C ₁	117.90	116.11	128.01	C ₁₂ -C ₁₁ -C ₁₀	122.20	121.03	120.93

Both of the ligands molecules are almost planers. Deviation from two plans comprising all non-H atoms: for the N3-ligand molecule, 0.041 Å°; for the N8 molecule, 0.092 Å°. The Mn-N bond lengths to the two ligands are comparable, averaging 2.30 Å° to the slightly longer bonds to the amine atoms and 2.21 Å° to the pyridine nitrogen atoms. These are comparable to $[\text{Mn}(\text{C}_9\text{H}_{11}\text{N}_3\text{O}_2)_2][2(\text{ClO}_4)^-]$. (avg. $\text{Mn-N}_{\text{oxime}}=2.29\text{Å}^\circ$; avg $\text{Mn-N}_{\text{pyr}}=2.18$,[21].

The perchlorate anion is not disordered at 293 K, and it is stabilized by strong interactions with its environment. The averages Cl-O bond distances; in the two perchlorate ions present in the asymmetric unit are 1.3555 Å° and 1.370 Å° respectively and the averages O-Cl-O bond angles are 109° and 109.3° (17), respectively, confirming a tetrahedral configuration , similar to other perchlorates studied at low temperature) [20, 22-24].

Due of the presence of two perchlorates (ClO_4^-) ions, the crystal pickings of the complex are mainly consolidate by N-H...O, O-H...O and C-H...O intra and intramolecular hydrogen bonds. Therefore, a total of eight hydrogen bonds are present in the unit (Figure.2) and (Table.5). Significant hydrogen bonds are formed between the oxime NH functions and the perchlorates ions to link molecules into parallel chaines (Figure.3).

Table 5. Hydrogen bond lengths (Å) and angles (°)

	D-H...A	D-H	H...A	D...A	D-H...A
N2	-- H2N .. O6	0.9300	2.0300	2.951(10)	172.00
N4	-- H4N .. O2	0.9000	2.4800	2.8436	105.00
N4	-- H4N .. O9 ⁱ	0.9000	2.1900	3.061(9)	161.00
N7	-- H7 .. O3	0.9000	2.5700	2.891(9)	102.00
N9	-- H9N .. O9	0.95(6)	2.45(6)	3.256(12)	143(5)
N9	-- H9N .. O12	0.95(6)	2.32(6)	3.187(15)	152(5)
C4	-- H4 .. O5 ⁱⁱ	0.9300	2.4500	3.135(10)	130.00
C12	-- H12 .. O5 ⁱⁱⁱ	0.9300	2.5500	3.359(13)	146.00

i : $[3/2-x, 1/2+y, 1/2-z]$; ii: $[1+x, y, z]$; iii: $[1/2-x, 1/2+y, 1/2-z]$

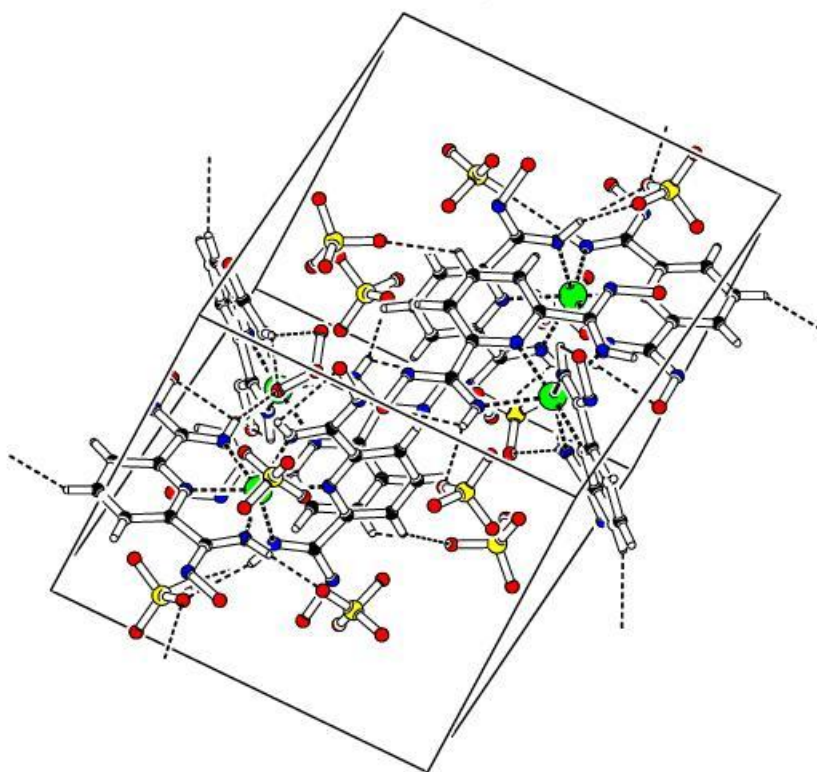


Fig.2. Crystal packing of the complex showing the H-bonding patterns

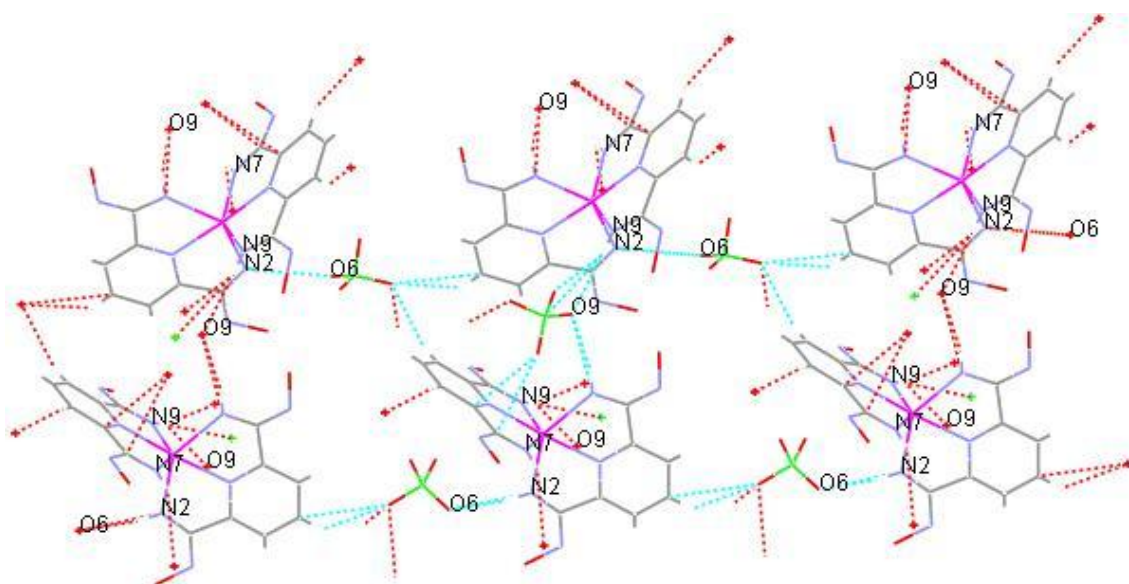


Fig.3. A fragment of the structure showing the hydrogen bonds as dashed lines

2.3 Fully optimizations

All the computations of mentioned complex were performed using the Gaussian 09 program

package [25] by means of the resources provided by GridChem Science Gateway [26]. GaussView 5.08 [27] was used for visualization of the structure and simulation of the vibrational spectra. Optimized structures of complex optimized using the DFT method with B3LYP functional in conjunction with the 6-31G(d, p) and lan12dz basis sets in the gas phase imposing the C1 and C2v symmetries. IR spectrum of this complex is calculated at same level of theory and examined in detail [28-30].

Table 1, Table 2 and figure.4 summarizes the optimized structure of manganese complex $[C_{14}H_{18}MnN_{10}O_4]^{2+}$ with different symmetries and its bond lengths and angles respectively. For $[C_{14}H_{18}MnN_{10}O_4]^{2+}$, the optimized bond distances and angles are well correlated with the X-ray bond parameters are given in (figure.4).

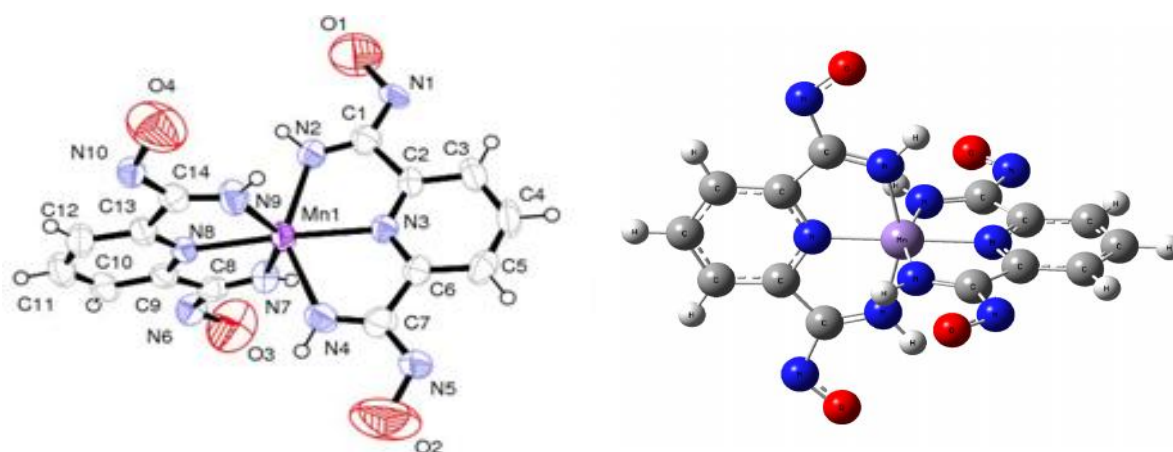


Fig.4. Ortep diagram of $[C_{14}H_{18}MnN_{10}O_4]^{2+}$ complex 50% probability thermal ellipsoids, showing the atomic numbering scheme and theoretically geometry optimization with C_{2v} symmetry for nominated complex by using DFT/UB3LYP method with LanL2DZ level.

According to Table 1 and Table 2, there are good agreements between experimental and calculated results. It is clear from these results there are very few differences between the optimized structure and the structure determined by the X-ray diffraction and the largest

difference between the experimental and calculated bond lengths and bond angles for the C_{2V} and C_1 symmetry with the lanl2dz level are respectively 0,05 Å and 0,1 Å (Mn-N) and 11,38 deg ,12,28 deg (N-Mn-N).

Distribution graphs between experimental and calculated results for bond lengths and bond angles are presented in Figure.5.

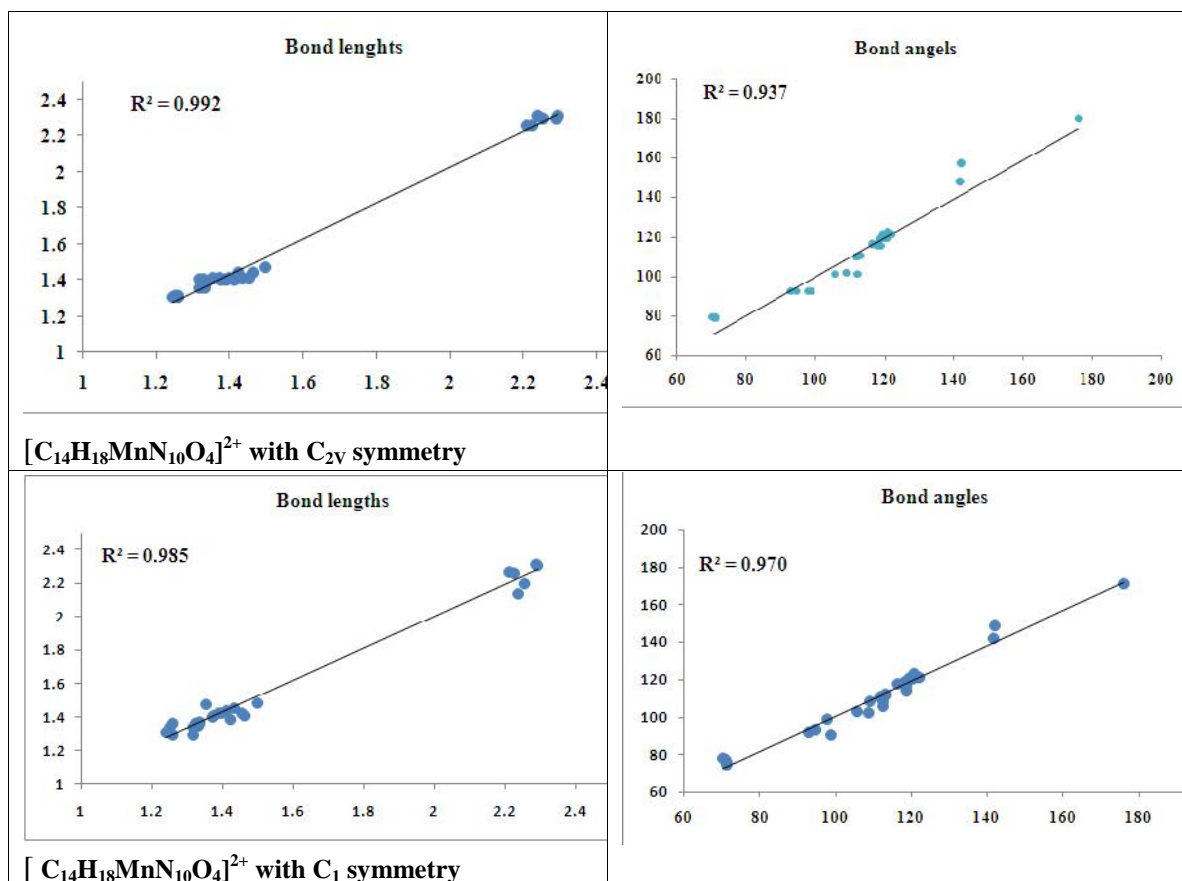


Fig.5. The distribution graphs between experimental and calculated results for $[C_{14}H_{18}MnN_{10}O_4]^{2+}$ in symmetries C_{2V} and C_1 respectively.

According to the Fig. 5, the correlation constants (R^2) are calculated for the C_{2V} and C_1 symmetries are respectively 0.992 and 0.985 for bond lengths and 0.937 and 0.97 for bond angles.

The IR spectrum of Mn(II) complex is calculated at the same level of theory and represented in Figure. 6.

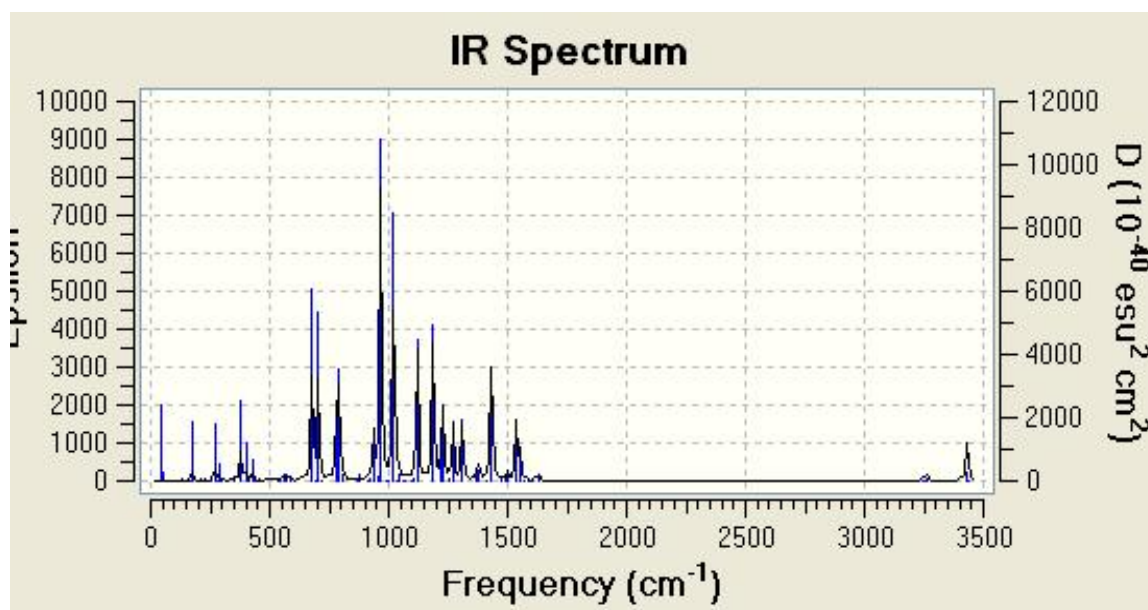


Fig.6. Calculated IR spectrum of Mn(II) complex with C_{2v} symmetry at DFT/UB3LYP/(LANL2DZ) level in vacuo.

Calculated stretching frequencies are obtained as: NH (3430 and 3433 cm^{-1}), CH (3244 – 3252 cm^{-1}), N=O (1534 cm^{-1}), C=N and C=C (1120 cm^{-1}), C=N in pyridine (966.62 cm^{-1}), Mn-N (677 and 399.39 cm^{-1}). These frequencies are not scaled and these are anharmonic frequencies and harmonic frequencies are scale by 0.961.

As for the values of the theoretical frequencies of vibration, there are all real and positive, indicating that the optimized structure corresponds to stationary state having a minimum of the hypersurface of the potential energy.

The diagrams of molecular orbitals and Contour plots of selected molecular orbitals of $[\text{C}_{14}\text{H}_{18}\text{MnN}_{10}\text{O}_4]^{2+}$ are summarized in figure.7.

Molecular orbitals (MOs) and their energy diagrams are important to determine the molecular properties. Especially, frontier molecular orbitals (FMOs) are playing important role in determination of chemical reactivity. Multiplicity of investigated compound is two in mentioned Mn complex. The energy diagrams from HOMO-2 to LUMO+2 are given in Figure. 7.

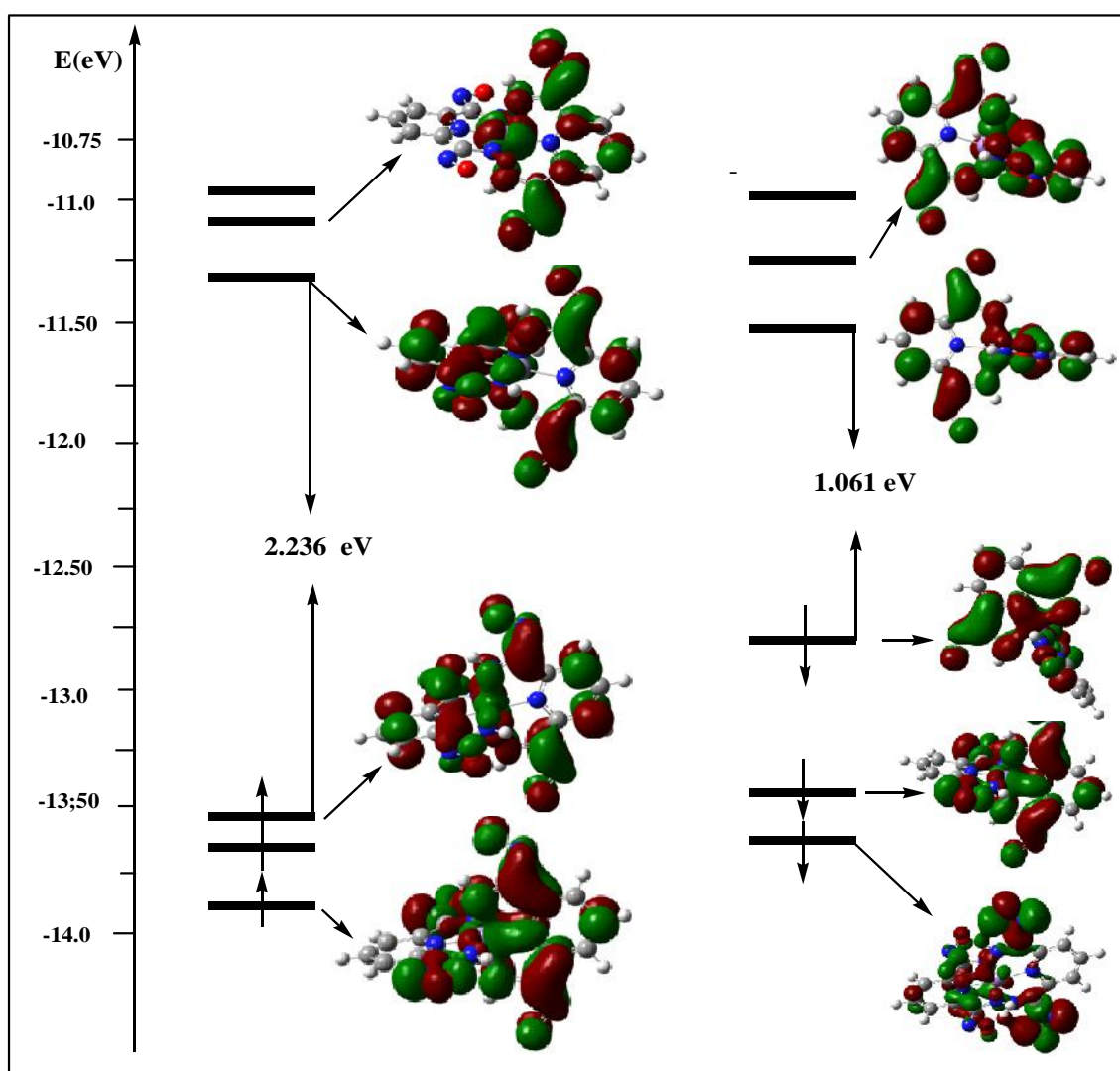


Fig.7. Molecular orbital energy diagrams from HOMO-2 to LUMO+2 and Contour diagrams of some orbital of mentioned Mn(II) complex at DFT/UB3LYP/LANL2DZ level in gas phase. The highest energy occupied molecular orbital (HOMO) and the lowest unoccupied molecular orbital (LUMO) of Mn complex are concentrated on the Mn atom and ligand and the

HOMO–LUMO energy gap is 2.236 eV and 1.06 eV for the α -spin and β -spin molecular orbitals respectively for the $[\text{C}_{14}\text{H}_{18}\text{MnN}_{10}\text{O}_4]^{2+}$ complex in the DFT/UB3LYP LanL2DZ level.

3. EXPERIMENTAL

3.1 Synthesis

2,6-Dicyanopyridine was synthesized from pyridine-2,6- dicarboxylic acid (Aldrich Chemical Co.) according to the procedure of Banks and Brookes [31].

3.1.1 Preparation of pyridine-2,6-diamidoxime, $\text{C}_7\text{H}_9\text{N}_5\text{O}_2$ (L)

50 cm³ of an aqueous hydroxylamine hydrochloride solution (1.215 g, 17.5 mmol) neutralized with sodium hydroxide (0.7 g, 17.5 mmol) was added to 50 cm³ of 2,6-dicyanopyridine (0.975, 7.5 mmol) dissolved in 50 cm³ of ethanol. The reaction mixture was heated at 70°C with stirring for 1 h, and upon cooling to 10°C yielded the ligand (L) (2.605 g, 89%), m.p. 213 °C . $\nu_{\text{max}}/\text{Cm}^{-1}$ (KBr disc): 3482 (asym) and 3414 (sym) (NH); and 3352 (sym) (OH); 1653 (sym) (C=N); 958 (sym) (NO). NMR $[(\text{CD}_3)_2\text{SO}; \delta\text{H}(250 \text{ MHz})$ 9.86 (s, 2 H, NO-H), 7.85 (m, AB₂, 3 H, pyridinering), 6.29 (s, 4 H, NH₂).

3.1.2 Preparation of bis(pyridine-2,6-diamidoxime)nickel(II) Perchlorate, $[\text{Mn}(\text{C}_7\text{H}_9\text{N}_5\text{O}_2)]^{2+}$, $2[\text{ClO}_4]^-$

50 cm³ of an aqueous solution of manganese (II) Perchlorate (0.655g, 5 mmol) was added to a heated alcoholic solution of the ligand (L) (0.725 g, 5 mmol). The resulting perchlorate solution was stirred at 40–50 °C for 1 h and allowed to stand 24 hours at room temperature.

The resulting pink crystals of (1) were filtered off and washed with absolute ethanol and diethyl ether.

3.2 Instrumentation

Using Mo K α radiation ($\lambda = 0.71073 \text{ \AA}$) in the range of $3.0 < 2\theta < 29.3^\circ$ at 293 K, a pink block selected crystal of the complex, with dimensions of $0.01 \times 0.02 \times 0.04 \text{ mm}^3$ was mounted on an Oxford Diffraction Xcalibur, Atlas, Gemini ultra diffractometer, equipped with the required cooling. The unit cell determination and data reduction were performed using the CrysAlis program [32]. A total of 13138 reflections were collected, of which 6163 were independent and

3734 reflections with $I > 2 \sigma(I)$. The structure was solved by direct methods using the program SIR2004 [33] and was refined by full-matrix least squares technique on F² including all reflections with SHELXL- 1997 program [34]. Both softwares were included within the WingX crystallographic software package [35].

All non-hydrogen atoms were anisotropically refined. All of the hydrogen atoms were located from the difference Fourier map and were fixed in calculated positions with distances constraints of C-H = 0.93 Å and

N-H = 0.86 Å, and refined in riding mode with $U_{iso}(H) = 1.2 U_{eq}(C,N)$. The refinements converged at conventional R factor of 0.0747 and wR of 13.17%. Structural representations of the complex were drawn using ORTEP-3 [36] and MERCURY [37]. Analyses were carried out by the program PLATON [38], as incorporated in the WinGX [39] pack.

The FTIR spectrums has been recorded in frequency region between 4000-400 cm^{-1} with a FTIR NEXUS NICOLET Spectrometer in KBr pellets.

The ^1H NMR has been recorded on a Bruker 300 MHz instrument at 23°C to confirm the molecular structure of our ligand.

Computational calculations were performed by using GaussView 5.0.8 [25] and Gaussian 09 AM64L-G09RevD.01 package program [26]. B3LYP functional was selected as computational method and LANL2DZ, 6-31G(d,p) levels where selected for the whole atoms in the molecule. Some stretching frequencies were selected from IR spectrum and these are examined in detail.

4. CONCLUSION

The experimental and theoretical structural investigations of an octahedral Mn(II) complex with oxime ligand were successfully performed by single-crystal XRD, the experimental values in the solid phase were recorded in the presence of intermolecular interactions. The theoretical study of the various properties structural, vibrational and electronic properties by means of the functional theory of the density (DFT) using the functional hybrid B3LYP at the 6-31G (d, p) and LanL2dz levels. To summarize, the following conclusions can be drawn:

1. The complex crystallizes in the monoclinic system, space group $P2_1/n$.

2. Crystals of the complex (1) suitable for X-ray study were grown from alcohol solution. Shows the expected 6-coordinate metal complex with two (L) ligands coordinated to the manganese ion, with a degree of distortion from an octahedral geometry.
3. The crystal structure of this complex shows the oxime nitrogens are not available for tridentate co-ordination in conjunction with the pyridine nitrogen.
4. The structure is held together through N-H...O and O-H...O and C-H...O hydrogen bonds occurring between the coordinated oxime molecules and the perchlorate counter-ions
5. Calculations concerning the optimization of the geometry (bond lengths and bond angles) have shown a good agreement between the results obtained by quantum chemical computations and experimental results the calculated lengths are slightly larger than those encountered in experimental data due to the fact the computations were performed for a single molecule in vacuo, where as the experimental values in the solid state
6. The vibration frequencies are all real for this complex, which implies that is a stationary state and the simplest spectrum is that which correspond to the highest symmetry.
7. The diagram of orbital molecular obtained by means of DFT/UB3LYP/6-31G (d, p) method showed that the bond gap energy HOMO-LUMO is important for the alpha and beta spin and the highest occupied molecular orbital has a sigma character.

5. SUPPLEMENTARY MATERIALS

CCDC 1401465 contains the supplementary crystallographic data for this paper. These data can be obtained free of charge via <http://www.ccdc.cam.ac.uk/conts/retrieving.html> (or from the Cambridge Crystallographic Data Centre, 12, Union Road, Cambridge CB2 1EZ, UK; fax: 00441223 336033).

6. ACKNOWLEDGEMENTS

This research is made possible by TUBITAK ULAKBIM, High Performance and Grid Computing Center (TR-Grid e-Infrastructure).

7. REFERENCES

- [1] Stamatatos TC, Escuer A, Abboud KA, Raptopoulou CP, Perlepes SP, Christou G. *Inorg Chem.* 2008, 47 (24), 11825-11838, DOI: 10.1021/ic801555e
- [2] Tschugaeff L. Ueber den Einfluss der Association der Flüssigkeiten auf das optische Drehungsvermögen derselben. *Chem. Ber.* 1898, 31 (2), 2451-2454
- [3] Wang B, Côté AP, Furukawa H, O'Keeffe M, Yaghi OM. *Nature.* 2008; 8;453(7192):207-11. doi: 10.1038/nature06900
- [4] Rocha J, Carlos LD, Almeida Paz FA, Ananias D. *Chem. Soc. Rev.* 2011, 40, 926–940, DOI: 10.1039/C0CS00130A
- [5] Chakravorty A. Structural chemistry of transition metal complexes of oximes. *oord. Chem. Rev.* 1974, 13(1), 1-46
- [6] Keeney M E, Osseo-Asare K, Woode K A. Transition metal hydroxyoxime complexes. *Coord. Chem. Rev.* 1984, 59, 141-201
- [7] Schrauzer GN. New developments in the field of vitamin B12: Reactions of the cobalt atom in corrins and in vitamin B12 model compounds. *Angew. Chem. Int. Ed. Engl.* 1976, 15:417-426
- [8] Kukushkin VY, Pombeiro AJL. Oxime and oximate metal complexes: unconventional synthesis and reactivity. *Coord. Chem. Rev.* 1999, 181(1):147-175
- [9] Biswas B, Salunke-Gawali S, Weyhermüller T, Bachler V, Bill E, Chaudhuri P. *Inorg Chem.* 2010, 49(2), 626-641, DOI: 10.1021/ic9018426
- [10] Jnan P N, Chiranjani B, Liping L, Miaoli Z. *J. Chem. Crystallogr.* 2011, 41,502–507, DOI 10.1007/s10870-010-9909-1
- [11] Costes J. P, Dahan F, Dupuis A. *J Chem Soc DaltonTrans.* 1998, (8), 1307- 1314 , DOI: 10.1039/A708374B
- [12] W.-K. Dong, Sh.-Sh. Gong, Y.-X. Sun, J.-F. Tong, and J. Yao. Structural characterisation of two copper (II) complexes with oxime-type ligands. *Journal of structural Chemistry.* 2011, 52(5) 1018-1024
- [13] Pearse G A, Raithby P R, Lewis J. Synthesis and X-ray crystal structure of pyridine-2-amidoxime, $C_6H_7N_3O$, and aqua-bis-(pyridine-2-amidoxime) copper (II) chloride, $[Cu(C_6H_7N_3O)(H_2O)]Cl_2$. *Polyhedron.* 1989, 8(3), 301-304

- [14] Pearse G A, Raithby P R, Hay C M , Lewis J. Synthesis and X-ray crystal structure of two complexes of nickel(II) nitrate with pyridine-2-amidoxime ($C_6H_7N_3O$): $[Ni(C_6H_7N_3O)_2(NO_3)_2]$ and $[Ni(C_6H_7N_3O)_3](NO_3)_2 \cdot H_2O$. *Polyhedron*. 1989, 8(3), 305-310
- [15] Nasakkala M, Saarinen H, Korvenranta J and Orama M. *Acta Crystallogr*. 1989, C 45: 1514-1517, doi:10.1107/S0108270189003331
- [16] Cullen D L. Liugafelten E C. *Inorg. Chem*. 1970, 9 (8), 1865-1877, DOI: 10.1021/ic50090a017
- [17] Pearse G A, Raithby P R, Maughan M M J. Synthesis and x-ray crystal structure of 2,2,2 -iminotris(acetamidoxime) copper(II) sulphate monohydrate. $[CuN(CH_2CNH_2: NOH)_3(SO_4)] \cdot H_2O$. *Polyhedron*. 1994, 13(4), 553-558
- [18] Pearse G A, Pfluger C E. The synthesis and crystal structure of ethylenedinitrilotetraacetamidoxime nickel(II) sulfate trihydrate. *Inorg Chim Acta*. 1994, 227(1), 171-174
- [19] Brad A B, George A P. J. *Chem. Soc . Dalton. Trans*. 1997, 2793–2797, DOI: 10.1039/A608599G
- [20] Hamdaoui A, Messai A, Benzya N. Lanez T, Sayin K. Synthesis, crystal structures, hydrogen bonding graph-sets and theoretical studies of nickel (+ii) co-ordinations with pyridine-2,6-dicarboxamide oxime. *J. Fundam. Appl. Sci.*, 2017, 9(1), 183-205.
- [21] Christopher W. Glynn and Mark M. Turnbull . Complexes of 2,6-diacetylpyridine dioxime (dapdoH₂). Crystal structures of $[M(dapdoH_2)_2](ClO_4)_2$ (M=Cu and Mn) . *Transition Metal Chemistry*. 2002, 27: 822–831
- [22] Messai A, Direm A, Benali-Cherif N, Luneau D, Jeanneau E. *Acta Cryst*. 2009, E65, o460, doi:10.1107/S1600536809003171
- [23] Bendjeddou L, Cherouana A, Dahaoui S, Benali-Cherif N, Lecomte C. *Acta Cryst*. (2003).E59(5),o649-o651, doi: 10.1107/S1600536803008080
- [24] Bendjeddou L, Cherouana A, Berrah F, Benali-Cherif N. *Acta Cryst*. (2003).E59(4),o574-o576, doi: 10.1107/S1600536803006457
- [25] M.J. Frisch, G.W. Trucks, H.B. Schlegel, G.E. Scuseria, M.A. Robb, J.R. Cheeseman, G. Scalmani, V. Barone, B. Mennucci, G.A. Petersson, H. Nakatsuji M. Caricato, X. Li, H.P.

Hratchian, A.F. Izmaylov, J. Bloino, G. Zheng, J.L. Sonnenberg, M Hada, M. Ehara, K. Toyota, R. Fukuda, J. Hasegawa, M. Ishida, T. Nakajima, Y. Honda, O. Kitao, H. Nakai, T. Vreven, J.A. Montgomery Jr., J.E. Peralta, F. Ogliaro, M. Bearpark, J.J. Heyd, E. Brothers, K.N. Kudin, V.N. Staroverov, R. Kobayashi, J. Normand, K. Raghavachari, A. Rendell, J.C. Burant, S.S. Iyengar, J. Tomasi, M. Cossi, N. Rega, J.M. Millam, M. Klene, J.E. Knox, J.B. Cross, V. Bakken, C. Adamo, J. Jaramillo, R. Gomperts, R.E. Stratmann, O. Yazyev, A.J. Austin, R. Cammi, C. Pomelli, J.W. Ochterski, R.L. Martin, K. Morokuma, V.G. Zakrzewski, G.A. Voth, P. Salvador, J.J. Dannenberg, S. Dapprich, A.D. Daniels, Farkas, J.B. Foresman, J.V. Ortiz, J. Cioslowski, D.J. Fox, Gaussian 09, Revision A.01, Gaussian, Inc., Wallingford CT, 2009.

[26] R. Dooley, K. Milfeld, C. Guiang, S. Pamidighantam, G. Allen. From Proposal to Production: Lessons Learned Developing the Computational Chemistry Grid Cyberinfrastructure. *J. Grid. Comput.* 2006, 4(2), 195–208.

[27] R.D. Dennington, T.A. Keith, J.M. Millam, GaussView 5.0.8, Gaussian Inc, 2008.

[28] K. Sayin, D. Karaka . Structural, spectral, NLO and MEP analysis of the $[\text{MgO}_2\text{Ti}_2(\text{OPr}^i)_6]$, $[\text{MgO}_2\text{Ti}_2(\text{OPr}^i)_2(\text{acac})_4]$ and $[\text{MgO}_2\text{Ti}_2(\text{OPr}^i)_2(\text{bzac})_4]$ by DFT method.

Spectrochimica Acta Part A: Molecular and Biomolecular Spectroscopy. 2015, 144, 176–182.

[29] M. Kurt, E. Babur Sas, M. Can, S. Okur, S. Icli, S. Demic, M. Karabacak, T. Jayavarthanam, N. Sundaraganesan. Synthesis and spectroscopic characterization on 4-(2,5-di-2-thienyl-1H-pyrrol-1-yl) benzoic acid: A DFT approach. *Spectrochimica Acta Part A: Molecular and Biomolecular Spectroscopy.* 2016, 152, 8–17.

[30] Fábio Balbino Miguel, Juliana Arantes Dantas, Stefany Amorim, Gustavo F.S. Andrade, Luiz Antônio Sodré Costa, Mara Rubia Costa Couri. Synthesis, spectroscopic and computational characterization of the tautomerism of pyrazoline derivatives from chalcones. *Spectrochimica Acta Part A: Molecular and Biomolecular Spectroscopy.* 2016, 152, 318–326.

[31] Banks R, Brookes R F. 2, 6-Dicyanopyridine: an improved preparation from pyridine-2, 6-dicarboxamide. *Chem. Ind.* 1974, 15, 617

[32] Oxford Diffraction (2006) Xcalibur CCD system, CrysAlis Software system, Version 1.171. Oxford Diffraction Ltd., Abington

- [33] Burla MC, Caliendo R, Camalli M, Carrozzini B, Cascarano G L, De Caro L, Giacovazzo C, Polidori G, Spagna R. *J. Appl. Crystallogr.* 2005, 38(2), 381–388, doi: 10.1107/S002188980403225X
- [34] Sheldrick GM (1997) SHELXL97. University of Goettingen, Germany
- [35] Farrugia L J. *J. Appl. Crystallogr.* 1999, 32(4), 837–838, doi:10.1107/S0021889899006020
- [36] Farrugia LJ. *J. Appl. Crystallogr.* 1997, 30(5), 565, doi: 10.1107/S0021889897003117
- [37] Bruno IJ, Cole J C, Edgington P R, Kessler . Macrae C F, McCabe P, Pearson J, Taylor R. *Acta.Cryst.* 2002, B58(3), 389–397, doi: 10.1107/S0108768102003324
- [38] Spek A L. *J. Appl. Crystallogr.* 2003, 36(1), 7-13, doi: 10.1107/S0021889802022112
- [39] GaussView, Version 5, Roy Dennington, Todd Keith, and John Millam, *Semichem Inc.*, Shawnee Mission, KS, 2009.

How to cite this article:

Benyza N, Messai A, Hamdaoui A, Lanez T and Sayin K. Synthesis, quantum chemical computations and x-ray crystallographic studies of a new complex based of manganese (+ii). *J. Fundam. Appl. Sci.*, 2017, 9(2), 770-789.